

pubs.acs.org/JPCC Article

Influence of Alkali Metal Cations on the Photodimerization of Bromo Cinnamates Studied by Solid-State NMR

Published as part of The Journal of Physical Chemistry virtual special issue "Hellmut Eckert Festschrift". Marufa Zahan, He Sun, Sophia E. Hayes, Harald Krautscheid, Jürgen Haase, and Marko Bertmer*



Cite This: J. Phys. Chem. C 2020, 124, 27614-27620



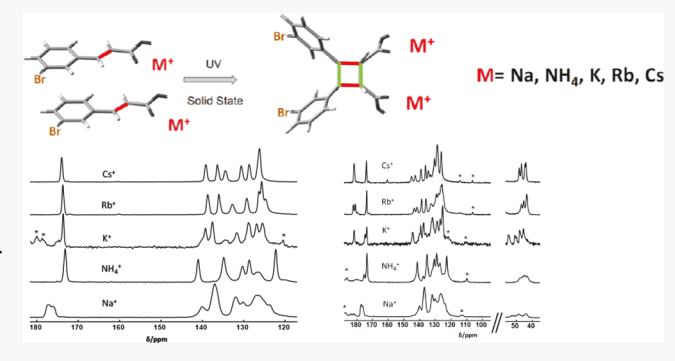
ACCESS

Metrics & More

Article Recommendations

Supporting Information

ABSTRACT: The alkali metal salts of *m*-bromocinnamic acid and their photodimerization products are analyzed by solid-state NMR. Cesium, rubidium, and potassium salts show well-resolved signals in the ¹³C CPMAS spectra, whereas for ammonium and sodium salts broader lines are obtained. The (size of the) cation and with that the packing arrangement in the crystal have a significant influence on the resulting spectra. With larger cations the chemical shift different between the two olefinic carbon signals gets smaller. One exception is the potassium salt which also shows a doubling of signals. All samples undergo [2 + 2] photodimerization upon irradiation with UV light to yield truxinates. Cesium, rubidium, and potassium salts show almost complete photoreaction, in



contrast to ammonium and sodium salts. Based on the signals for cyclobutane carbons, a nonplanar ring is present in all samples.

■ INTRODUCTION

Solid-state photoreactions are particularly interesting in stereoselective synthesis. As the molecular arrangement of reacting molecules is fixed by the crystal structure, predominantly stereoselective products are obtained that require a minimum displacement of atoms. The reactions also follow the concept of supramolecular chemistry. Furthermore, such reactions are also environmentally friendly as no solvent is needed and—in the case of quantitative reaction—no work-up step is required.

A common organic solid-state reaction in this regime is the (intermolecular) [2 + 2] photodimerization applicable for alkenes like coumarins, stilbenes, or anthracenes.^{4,5} For photoreactive molecules that are stable as both reactant and product, and where the photoreaction is reversible, there are also potential applications as molecular switch or molecular memory.^{6,7}

A prominent [2+2] photodimerization reaction is that of cinnamic acid. Schmidt and co-workers^{8–11} investigated a series of *trans*-cinnamic acids and laid the basis of the topochemical principle^{11,12} for these types of reactions. This principle states that reactivity is governed by the packing of molecules, especially the distance of reacting double bonds and their relative orientation. With that reactions progress with a minimum displacement of atoms.

Cinnamate groups have also been used for different purposes, such as side groups in polymers to be used for crack healing. The photoreversibility has also been demonstrated. Here, photodimerization takes place at longer

wavelengths, typically above 260 nm. The breaking of the cyclobutane ring then happens with UV light below (shorter than) 260 nm. This concept has also been employed with cinnamic acid as side chains in polymers, ¹⁵ including shapememory polymers. ¹⁶

The cinnamic acid photodimerization is a fairly simple model system that can be well analyzed by solid-state NMR as has been demonstrated previously. ^{17–22} In our approach to study the variation of the molecular arrangement and its influence on photodimerization, we prepared cinnamate salts with various alkali cations. The photodimerization reaction is illustrated schematically in Scheme 1 for the example of *m*-bromo cinnamate to truxinate, showing the head-to-head packing in the crystal starting material.

In this contribution, we have employed ¹³C solid-state NMR spectroscopy as an element-selective, noninvasive technique. NMR can identify side products and also noncrystalline materials besides the crystalline components. The chemical shifts are influenced by the local electronic environment of bonding orbitals that are also influenced by packing effects and other intermolecular interactions. We characterize both

Received: October 31, 2020 Revised: November 23, 2020 Published: December 4, 2020





Scheme 1. Photodimerization of Cinnamate Salts

reactants and photoproducts. Comparison with crystal structures and theoretical calculations is done, and results are correlated to cation size.

EXPERIMENTAL SECTION

Sample Preparation. *trans-m*-Bromocinnamic acid (98%), hydroxides of ammonium, sodium, potassium, rubidium, and cesium as well as ethanol were all obtained from Sigma-Aldrich. All chemicals were used as purchased. The preparation of ammonium and potassium salts is described in the literature. The acid is dissolved in ethanol and the alkali hydroxides in water. The hydroxide solution is slowly mixed into the acid solution, and the solvent is allowed to evaporate slowly for crystallization. This procedure was then also adapted for the other alkali cinnamates. Evaporation took place in the dark to prevent inadvertent photoreaction. We use a short notation to identify the different salt samples. For example, potassium *m*-bromocinnamate is named KBrCin, and the corresponding photoproduct is named KBrTrux.

Photoirradiation. The cinnamate samples were irradiated by using a 100 W HP Hg lamp (HBO, Osram) which emits a broad range of wavelengths from UVC to the visible range. A UV-enhanced aluminum mirror (Thorlabs PF 10-03-F01) was used for reflecting the UV radiation from the lamp to the sample. This mirror provides more than 90% reflectance from 250 to 450 nm. The emission spectrum of the lamp was measured by a Maya 2000 UV—vis spectrometer from Ocean Optics (spectrum shown in the Supporting Information, Figure S1). The solid-state absorption spectrum of KBrCin powder for example shows that the absorption maximum is in the 250–300 nm wavelength range (spectrum included in Figure S1).

For irradiation with UV light, the samples were spread on small Petri dishes as thin layers and placed in the focus of the UV light reflected from the mirror. The sample temperature was maintained at room temperature (21 \pm 2 °C) without additional cooling. All samples were irradiated for successive irradiation periods, and the powders were stirred between each consecutive period of 1 h to irradiate the samples uniformly.

Solid-State NMR Measurements. Solid-state MAS NMR experiments were conducted on either a Bruker Avance 750 (17.6 T) or a Bruker Avance III HD 500 (11.74 T) spectrometer with a 4 mm MAS probe at rotation frequencies of 8–12 kHz. ¹³C CPMAS²⁶ experiments were executed at 188.35 and 125.75 MHz, respectively. Contact times were 2 ms unless stated otherwise, and TPPM²⁷ or SPINAL64^{28,29} were used for ¹H decoupling. Recycle delays were in the range 30–300 s, differing for each salt. The dipolar dephasing³⁰ experiments to detect only signals from nonprotonated carbons with decoupling partially off were recorded on a Bruker Avance 400 spectrometer with frequencies of 400.13 and 100.63 MHz for ¹H and ¹³C, respectively, also using a 4

mm MAS probe. All measurements were done at room temperature.

Two-dimensional FSLG-HETCOR (frequency-switched Lee–Goldburg heteronuclear correlation)³¹ experiments were conducted with the Bruker Avance 750 spectrometer at room temperature at 10 kHz MAS with a cross-polarization contact time of 0.5 ms, a recycle delay of 20 s, 128 t_1 increments with 100 scans, and rf field strengths of 172 and 125 kHz for ¹³C and ¹H, respectively. The ¹H 90° pulse length was 4 μ s, and SPINAL64 was used for proton decoupling during acquisition.

All spectra were referenced to tetramethylsilane (TMS) by using tyrosine hydrochloride as a secondary reference for ¹³C. Spectrum deconvolution was performed by using the dmfit software.³²

Computational Methods. DFT-NMR calculations were performed on CsBrCin and KBrCin with the CASTEP³³ package within the Perdew–Burke–Ernzerhof (PBE) generalized gradient approximation (GGA) formulation of the exchange-correlation energy. "On the fly" generated ultrasoft pseudopotentials were used to approximate the interaction between the core electrons and the nuclei. The cutoff energy of the plane-wave basis set was 630 eV, and the Monkhorst–Pack grid³⁴ sampling the Brillouin zone was chosen with *k*-point separation of 0.05 Å⁻¹. Energy calculations with and without geometry optimization were performed and compared with each other. Geometry optimization significantly reduces the remaining stress on the structure, and the corresponding calculated NMR tensor is closer to experiment.

■ RESULTS AND DISCUSSION

¹³C CPMAS Spectra of Cinnamate Salts. Figure 1 represents the isotropic part of the ¹³C NMR spectra of the

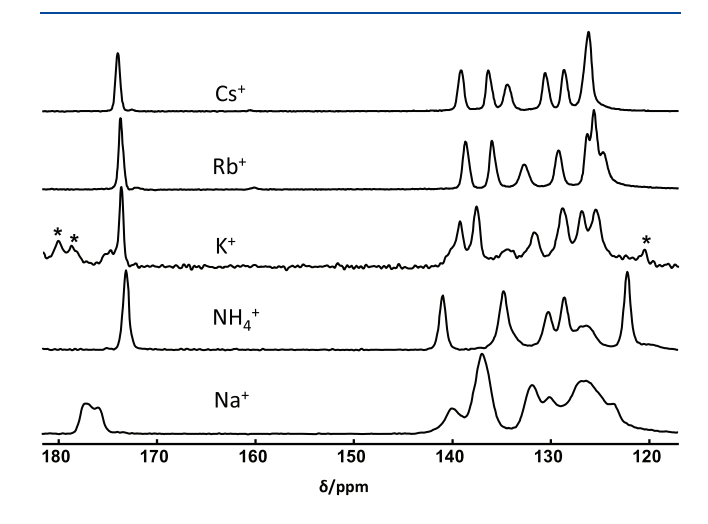


Figure 1. Stack plot of the isotropic part of the ¹³C CPMAS spectra of *m*-bromo cinnamate salts for different cations. The asterisks mark spinning sidebands.

different cinnamate salts. It can be seen that although the same anion is present in all samples, there are significant differences when varying the alkali cation. Additionally, different line widths (especially seen for NaBrCin) are apparent that indicate different local symmetry and degree of order for the different salts. As the sodium salt exhibits poor resolution together with two signals for the carboxylate carbon at higher chemical shift values, it is excluded from the following discussion.

The crystal structures of KBrCin and NH_4BrCin are published in ref 23 and 24. For the rubidium and cesium analogues the crystal structure has been determined in this study (see the Supporting Information). In every structure, a head-to-head arrangement of two anions, the " β " form, is present that results in the formation of truxinate dimers after photoreaction. There is no crystal structure existing for NaBrCin, and we were not able to get suitable crystals for X-ray diffraction. As can be seen in Figure 1, the ¹³C spectrum of the sodium salt is characterized by larger line widths compared to the other samples which is probably due to structural disorder.

Scheme 2 shows the numbering of carbon atoms for the cinnamate anion; the assignments are summarized in Table 1.

Scheme 2. Carbon Numbering Used for All Samples

M = Na, NH₄, K, Rb, Cs

The signal for carbon 3, bound to bromine, is hardly detectable among the other signals because of second-order quadrupolar effects, 35 which has been seen also for bromocinnamic acids. 20

Table 1. Assignment of ¹³C Isotropic Chemical Shifts for Different m-Bromo Cinnamate Salts^a

carbon no.	Na	NH ₄	K^{b}	Rb	Cs	acid
C1	137.0	134.8	137.7, 138.4	136.0	136.0	134.0
C2 ^c	126.4	125.9	125.5, 125.7	125.8	126.4	130.0
C4 ^c	131.9	130.2	134.5, 136.4	132.8	134.5	133.0
C5 ^c	130.2	128.7	131.7, 132.7	129.4	130.6	130.0
C6 ^c	126.9	126.6	128.9, 130.2	126.4	128.6	133.0
C7	140.0	141.0	139.3, 140.3	138.7	139.2	146.0
C8	123.8	122.3	126.9, 127.7	124.7	126.0	117.0
C9	177.3, 175.8	173.2	173.7, 174.8	173.8	174.0	174.0

"Carbon numbering as shown in Scheme 2. For comparison, also the shifts for *m*-bromocinnamic acid ("acid") are given. ²⁰ ^bFor doubling of signals, see the discussion (2D ¹³C-¹H HETCOR) below. ^cAssignment of protonated aromatic carbons was made in accordance with CASTEP results (see below).

This site is therefore not included in the table. Assignments were aided by short contact time and dipolar dephasing spectra (see Figures S2–S6) together with comparison to previous works²⁰ and results from CASTEP calculations. The deconvolution of each salt spectrum is shown in Figures S7–S11.

Surprisingly, apart from the sodium salt, the carboxylic carbon (C9) shows almost no variation in shift with cation. The shift is also very similar to that of the (protonated) acid form. In contrast to this, the signals for the vinyl carbons (C7, C8) show larger variations among the samples and are especially different from that of the acid form. For C8, shifts to higher ppm values between 5 and 10 ppm compared to the acid are found, and for C7 between 5 and 8 ppm shifted to lower values. Because of this, the signals move closer together with increasing cation size compared to the acid, with the ammonium sample being closest to the acid in shift values.

For the aromatic carbons, there is a general increase of shift with increasing cation size, especially striking for carbon number 4 next to the carbon bound to bromine. For the others, the shift differences are fairly small. One exception is the potassium salt which generally shows larger shift values than expected from the general trend. It has to be mentioned, though, that the assignment of protonated aromatic carbons is not unambiguous. We just followed the assignment that carbon atom 2 has the smallest and carbon atom 4 the largest shift (see also discussion below).

To get further insights into the origin of the observed ¹³C shifts, Figure 2 shows the geometric arrangement of the two

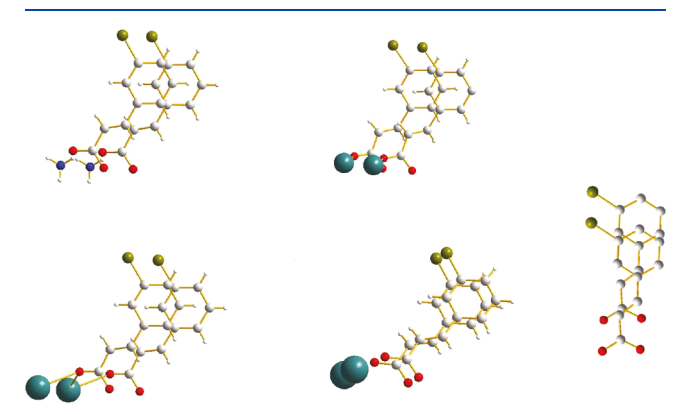


Figure 2. Sketch of the two reacting cinnamate anions for NH₄BrCin (top left), 23 KBrCin (top middle), 24 RbBrCin (bottom left), and CsBrCin (bottom middle) according to crystal structure data. For comparison, the corresponding representation for *m*-bromocinnamic acid is added on the right. In all cases the viewing direction is perpendicular to the aromatic ring. Color notation: C, gray; O, red; Br, olive; H, white; N, blue; alkali metal, turquoise. For the structures of RbBrCin and CsBrCin see the Supporting Information.

neighboring anions that can dimerize in the respective salts and the free acid from the crystal structures. The structures are rendered in a way that both aromatic rings are parallel with respect to each other, viewed along the normal of the ring plane. Most strikingly is the difference in arrangement of the anions in comparison to the free acid. Whereas in the salts, a sideways displacement of aromatic rings is observed, for the free acid there is a small shift lengthwise along the longer dimension of the *m*-bromocinnamic acid. Still, in all samples a suitable arrangement of the double bonds for photodimerization exists. Among the salts, the cesium compound shows only

a small displacement of the aromatic rings compared to NH_4 , K, and Rb salts. The distance between neighboring aromatic rings does not show a systematic variation with cation size, being similar for all, and therefore does not seem to have an effect on the observed ^{13}C shifts.

Further verification of our analysis is done by theoretical calculation of the ¹³C shifts with the CASTEP program. For this, computations of the cesium salt and the potassium salt were successful; the latter is interesting because it shows doubling of signals. The shifts are tabulated in Tables S3 and S4 together with a graphical comparison to the experimental data (Figures S12 and S13). The agreement is very good (rmsd = 1.29 ppm for the cesium and rmsd = 1.50 for the potassium salt) with the exception of the carbon atom next to bromine. This was also observed for other bromine-containing cinnamic acid derivatives.²⁰ The assignments from the calculation were also used as a guide for the signal assignment of the other salt samples. For KBrCin there are two molecules in the asymmetric unit. However, the corresponding ¹³C shifts are very similar and cannot be resolved experimentally.

Figure S14 shows the aromatic region of the 2D HETCOR spectrum of KBrCin, revealing that every signal is effectively a superposition of two signals with similar shift, of which only the signal (assigned to C4) near 135 ppm shows a fairly good separation of the two signals. The potassium sample therefore shows polymorphism, and we attribute the doubling of signals to small displacements between cinnamate ions. The deconvolution (Figure S9) leads to two groups of signals with the one group being more intense than the other. The more intense peaks agree well with the CASTEP results based on the single crystal structure data. The other polymorph could not be isolated.

¹³C CPMAS Spectra of Truxinates. For the photoproducts no crystal structures are available so we have to base our analyses on the ¹³C solid-state NMR spectra of the photoproducts in comparison to the reactant spectra. Figure 3 shows a stack plot of the ¹³C CPMAS spectra of *m*-bromo

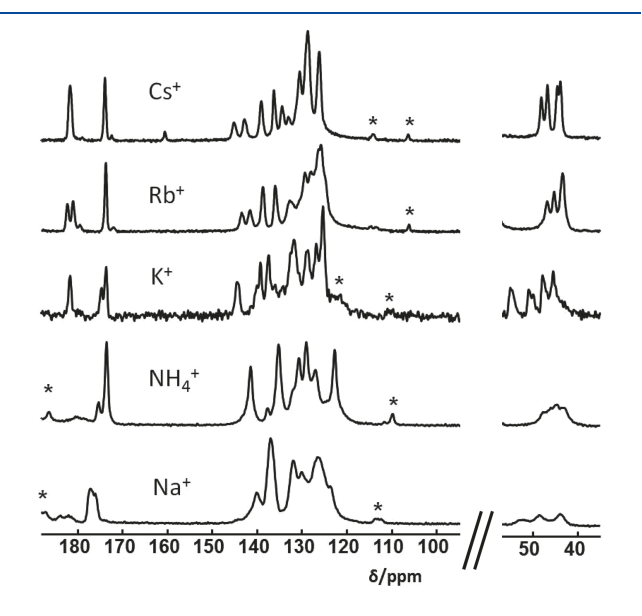


Figure 3. Stack plot of the relevant parts of the ¹³C CPMAS spectra of partially reacted *m*-bromo cinnamate salts to *m*-bromo truxinates with various cations after irradiation (Na 45 h, NH₄ 15 h, K 10 h, Rb 8 h, Cs 20 h). Asterisks mark spinning sidebands.

cinnamate salts with various cations after different total photoirradiation times. We show partially reacted samples after different reaction times where signals from reactant and photodimer can be seen together in significant amounts. With this, one can directly see the newly emerging signals, that is, the cyclobutane signals around 40–50 ppm as well as the carboxylate carbon signal around 180 ppm and the non-protonated aromatic (ipso) carbon signal at 140–145 ppm. For the other aromatic signals the signal overlap prevents simple assignment. The fact that no additional signals are present in significant amounts indicates that no side products are present. In all cases, more than two signals for the cyclobutane carbons indicate lower symmetry and hence a nonplanar ring.

The chemical shifts of the neighboring carbons, that is, the ipso (nonprotonated aromatic) carbon and the carboxylic carbon from the photoproduct, show a shift to higher ppm values due to the differing inductive effects of the reactant vinyl and product cyclobutane carbons. Tentative assignments are given in Table S5. For these, also dipolar dephasing and short contact time measurements were used to confirm assignments. Figures S15–S17 show the results for cesium, rubidium, and potassium truxinates. Deconvolution of the different truxinate spectra is given in Figures S18–S22.

In the case of a nonplanar ring, two signals each for carboxylic and ipso carbon atoms are expected, which is also seen for the rubidium sample. For the cesium compound, two ipso and one carboxylic signal are found. However, the width of the latter is larger than that of the other signals so that there are in fact two signals with very similar shifts present. For the potassium salt, only one signal each is found so that there is only a small or no chemical shift difference between the two. Nevertheless, the clear observation of four cyclobutane signals indicates a nonplanar ring (see also comment below). For the ammonium and sodium samples, the larger line width of signals prevents a clear assignment. We note that while the reactant of the ammonium salt shows fairly good resolution, this is not true for the photoproduct. For sodium, both reactant and product show large line widths that complicate analysis. In both cases, the large line widths arising from slight variations in chemical shifts for an individual carbon atom can be explained by a structural disorder showing different bond distances and bond angles.

From the relative intensities of either the vinyl and cyclobutane signals or alternatively the separated carboxylate signals of reactant and product, one can determine the degree of conversion (see below).¹⁷ More details on the reaction kinetics and factors that influence it will be discussed in an upcoming publication.³⁷ The ¹³C CPMAS spectra of CsBrCin and its photoproduct after 215 h of irradiation are compared in Figure 4. There is some intensity for the cinnamate remaining; a deconvolution of the truxinate is shown in Figure S18. The degree of conversion is 83% and cannot be increased with further irradiation. In a related study of halogen-substituted trans-cinnamic acid³⁸ incomplete photodimerization was also observed. This was explained with a theoretical model by Savion and Wernick³⁹ by the creation of isolated monomers during reaction. This model predicts a degree of conversion of 86%, close to our observation. Why this result is observed for the cesium salt and not for the other salts (see below) is not understood. For different cinnamic acids, we observed quasifull conversion. 17-20

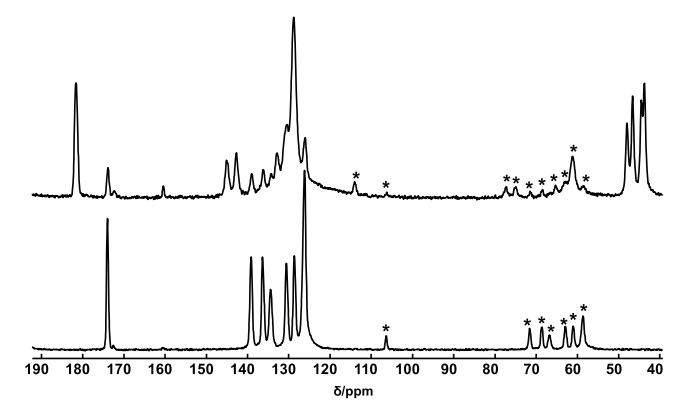


Figure 4. Comparison of ¹³C CPMAS spectra of CsBrCin (bottom) and CsBrTrux after 215 h of irradiation (top). The degree of conversion is 83%. Asterisks mark spinning sidebands, and the spinning frequency is 8.5 kHz.

Results for rubidium and potassium salts are shown in Figures 5 and 6, respectively. For the rubidium sample, almost

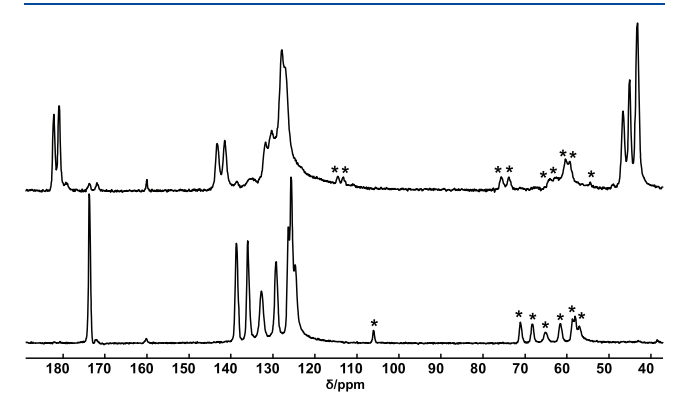


Figure 5. Comparison of ¹³C CPMAS spectra of RbBrCin (bottom) and RbBrTrux after 215 h of irradiation (top). The degree of conversion is 93%. Asterisks mark spinning sidebands; the spinning frequency is 8.5 kHz.

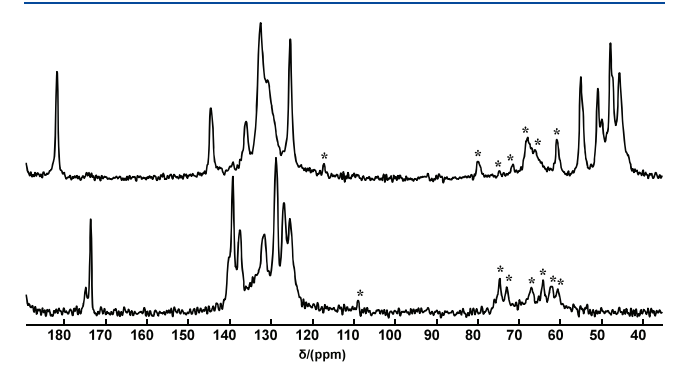


Figure 6. Comparison of ¹³C CPMAS spectra of KBrCin (bottom) and KBrTrux after 87 h of irradiation (top). The degree of conversion is 96%. Asterisks mark spinning sidebands, and the spinning frequency is 8.5 kHz.

full reaction is achieved after 215 h, with a calculated degree of conversion of 97%. There are three cyclobutane carbons observed; however, one of them has almost double intensity, also representing contributions from four cyclobutane signals as expected for a nonplanar ring. Compared to the reactant, a slight increase in line width is observed, indicating a lower

degree of crystallinity for the rubidium truxinate. Also for the potassium sample, almost full reaction is observed after 87 h of irradiation, about 96% conversion. Also here, lines are broadened for the truxinate compared to the cinnamate. In all three cases, the signals of the aromatic carbons (except the ipso carbon) are merged together compared to the reactant cinnamates. Therefore, assignments as given in Table S5 are merely tentative for the aromatic carbons.

The polymorphism of the potassium sample is also found in the photoproduct. Two pairs of four cyclobutane signals can be identified. This can be best seen in the $2D^{13}C^{-1}H$ HETCOR spectrum (Figure S23), where the second dimension helps resolve overlapping signals. Apart from the signals at 50/51 ppm, the doubling of signals is visible as a shoulder only in the one-dimensional spectrum. The HETCOR spectrum recorded with a long contact time also reveals correlation signals of cyclobutane protons and photoproduct carboxylic and ipso carbons next to the cyclobutane ring. We conclude from these data that the two polymorphs are very similar, and both photoreact. They also seem to be comparable in reactivity based on the similarity and intensity of product formation.

The ¹³C CPMAS spectra of NH₄BrCin after 32 h of irradiation and NaBrCin after 130 h irradiation are shown in Figures S21 and S22, respectively, together with the signal deconvolution. In both cases the signal intensity in the range 40-55 ppm indicates that photodimerization occurred. However, the larger line width of the signals—probably due to low crystallinity—complicates a clear assignment. Furthermore, the fact that only a maximum of 40% conversion could be achieved means that these systems are not well suited for solid-state photoreaction. In our view, this is primarily due to the lower degree of order that prevents progression of the reaction. For the ammonium sample, from the crystal structure suitable conditions for a photoreaction (appropriate distance between reacting double bonds and almost parallel alignment) exist which should allow for good photoreaction. For the sodium sample, the source of disruption to truxinate formation remains unknown.

Finally, to confirm formation of truxinates for all samples the solids were dissolved and characterized. The ¹³C NMR spectra of the different salts in solution (DMSO, not shown) all reveal two cyclobutane carbons, each corresponding to a planar ring in solution as expected. Furthermore, in ¹H NMR spectra, the two pairs of protons from the cyclobutane ring are doublets with a *J*-coupling of about 6 Hz as found also in other cyclobutanes with similar substitution. ⁴⁰ This verifies the head-to-head arrangement for all samples leading to truxinates.

CONCLUSION

We studied the influence of alkali metal cations in *m*-bromo cinnamate salts on their crystal structures and by that on the ¹³C CPMAS solid-state NMR spectra. For the different carbon atoms only small variations or a (slight) increase in chemical shift with cation size is observed. Exceptional is the potassium salt which shows higher shifts than expected and also polymorphism in both reactant and photoproduct. Salts with potassium, rubidium, and cesium show well-resolved spectra, whereas for ammonium and especially sodium, low resolution is found. This is probably relating to the degree of crystallinity; for the sodium sample, no crystal structure determination was possible. Verification of the ¹³C NMR assignments was performed by CASTEP calculations for the cesium and potassium salts, which showed very good agreement. The

combination of solid-state NMR, crystal structures, and theoretical calculations therefore allows for a detailed description of the alkali cinnamates.

All herein studied cinnamate salts undergo photodimerization in the presence of UV irradiation. In all cases truxinates result based on the head-to-head arrangement of the reacting monomers. Whereas in solution, a planar cyclobutane ring exists, nonplanar rings are present for all photoproducts in the solid state. Overall, the results show the significant influence of the cation on both NMR spectra and photodimerization even with similar structures and intermolecular spacings.

ASSOCIATED CONTENT

Supporting Information

The Supporting Information is available free of charge at https://pubs.acs.org/doi/10.1021/acs.jpcc.0c09826.

Crystal structure data of RbBrCin and CsBrCin; UV—vis spectrum of KBrCin and emission spectrum of the 100 W Hg lamp; ¹³C CPMAS short contact and dipolar dephasing NMR spectra; deconvolution of ¹³C CPMAS spectra; CASTEP results for CsBrCin and KBrCin; 2D HETCOR spectra of KBrCin and KBrTrux; ¹³C signal assignments of truxinate salts (PDF)

AUTHOR INFORMATION

Corresponding Author

Marko Bertmer — Felix Bloch Institute for Solid State Physics, Leipzig University, Leipzig, Germany; oorcid.org/0000-0002-3208-7927; Email: bertmer@physik.uni-leipzig.de

Authors

Marufa Zahan — Felix Bloch Institute for Solid State Physics, Leipzig University, Leipzig, Germany

He Sun − Department of Chemistry, Washington University in St. Louis, St. Louis, Missouri 63130, United States;
ocid.org/0000-0002-1887-1643

Sophia E. Hayes — Department of Chemistry, Washington University in St. Louis, St. Louis, Missouri 63130, United States; occid.org/0000-0002-2809-6193

Harald Krautscheid — Institute for Inorganic Chemistry, Leipzig University, Leipzig, Germany; orcid.org/0000-0002-5931-5440

Jürgen Haase – Felix Bloch Institute for Solid State Physics, Leipzig University, Leipzig, Germany; orcid.org/0000-0002-0140-6964

Complete contact information is available at: https://pubs.acs.org/10.1021/acs.jpcc.0c09826

Notes

The authors declare no competing financial interest.

■ ACKNOWLEDGMENTS

We thank Prof. Jörg Matysik, Analytical Chemistry, Leipzig University, for allowing us to use his HP lamp to perform the photoreactions. We thank the German Research Foundation (DFG) for funding (BE 2434/4-3). This work is supported (for H.S. and S.E.H.) by the U.S. National Science Foundation (NSF) Award 1640899.

REFERENCES

- (1) Zhu, B.; Wang, J.-R.; Zhang, Q.; Mei, X. Greener solid-state synthesis: stereo-selective [2+2] photodimerization of vitamin K_3 controlled by halogen bonding. CrystEngComm **2016**, 18, 6327–6330.
- (2) Ortega, G.; Briceño, A. Template-stereocontrolled [2 + 2] photoreactions directed by surface recognition on hydrophilic functionalized carbon materials. *CrystEngComm* **2018**, *20*, 2932–2939
- (3) Lehn, J.-M. Supramolecular Chemistry; VCH: Weinheim, 1995.
- (4) Ramamurthy, V.; Venkatesan, K. Photochemical reactions of organic crystals. *Chem. Rev.* **1987**, *87*, 433–481.
- (5) Tanaka, K.; Toda, F. Solvent-free organic synthesis. *Chem. Rev.* **2000**, *100*, 1025–1074.
- (6) Feringa, B. L.; Huck, N. P. M.; Schoevaars, A. M. Chiroptical Molecular Switches. *Adv. Mater.* **1996**, *8*, 681–684.
- (7) Dvornikov, A. S.; Liang, Y.; Cruse, C. S.; Rentzepis, P. M. Spectroscopy and Kinetics of a Molecular Memory with Non-destructive Readout for Use in 2D and 3D Storage Systems. *J. Phys. Chem. B* **2004**, *108*, 8652–8658.
- (8) Cohen, M.; Schmidt, G. 383. Topochemistry. Part I. A survey. *J. Chem. Soc.* **1964**, 1996–2000.
- (9) Cohen, M. D.; Schmidt, G. M. J.; Sonntag, F. I. Topochemistry. Part II. The Photochemistry of trans-Cinnamic Acids. *J. Chem. Soc.* **1964**, 2000–2013.
- (10) Schmidt, G. M. J. Topochemistry. Part III. The Crystal Chemistry of some trans-Cinnamic Acids. *J. Chem. Soc.* **1964**, 2014–2030
- (11) Schmidt, G. Photodimerization in the solid state. *Pure Appl. Chem.* 1971, 27, 647–678.
- (12) Cohen, M. D. Photochemie organischer Festkörper. Angew. Chem. 1975, 87, 439–447.
- (13) Chung, C.-M.; Roh, Y.-S.; Cho, S.-Y.; Kim, J.-G. Crack Healing in Polymeric Materials via Photochemical [2 + 2] Cycloaddition. *Chem. Mater.* **2004**, *16*, 3982–3984.
- (14) Akabori, S.; Habata, Y.; Nakazawa, M.; Yamada, Y.; Shindo, Y.; Sugimura, T.; Sato, S. The novel syntheses of photoreversible cyclobutanocrown ethers by the intramolecular photoaddition of α , ω -dicinnamoyl polyethylene glycol derivatives. *Bull. Chem. Soc. Jpn.* **1987**, *60*, 3453–3455.
- (15) Nakayama, Y.; Matsuda, T. Preparation and characteristics of photocrosslinkable hydrophilic polymer having cinnamate moiety. *J. Polym. Sci., Part A: Polym. Chem.* **1992**, *30*, 2451–2457.
- (16) Lendlein, A.; Jiang, H.; Jünger, O.; Langer, R. Light-induced shape-memory polymers. *Nature* **2005**, 434, 879–882.
- (17) Bertmer, M.; Barnes, A. B.; Nieuwendaal, R. C.; Hayes, S. E. Solid-State Photodimerization Kinetics of α -trans-Cinnamic Acid to α -Truxillic Acid Studied via Solid-State NMR. *J. Phys. Chem. B* **2006**, 110, 6270–6273.
- (18) Fonseca, I.; Hayes, S. E.; Blümich, B.; Bertmer, M. Temperature stability and photodimerization kinetics of β -cinnamic acid and comparison to its α -polymorph as studied by solid-state NMR spectroscopy techniques and DFT calculations. *Phys. Chem. Chem. Phys.* **2008**, *10*, 5898–5907.
- (19) Fonseca, I.; Hayes, S. E.; Bertmer, M. Size effects of aromatic substitution in the *ortho* position on the photodimerization kinetics of α -trans cinnamic acid derivatives. A solid-state NMR study. *Phys. Chem. Phys.* **2009**, *11*, 10211–10218.
- (20) Fonseca, I.; Baias, M.; Hayes, S. E.; Pickard, C. J.; Bertmer, M. Effects of Aromatic Substitution on the Photodimerization Kinetics of β -trans Cinnamic Acid Derivatives Studied with ¹³C Solid-State NMR. *J. Phys. Chem. C* **2012**, *116*, 12212–12218.
- (21) Harris, K. D.; Thomas, J. M. Probing polymorphism and reactivity in the organic solid state using ¹³C NMR spectroscopy: studies of p-formyl-trans-cinnamic acid. *J. Solid State Chem.* **1991**, *94*, 197–205.
- (22) Khoj, M. A.; Hughes, C. E.; Harris, K. D. M.; Kariuki, B. M. Polymorphism in a *trans*-Cinnamic Acid Derivative Exhibiting Two Distinct β -type Phases: Structural Properties, [2 + 2] Photo-

- dimerization Reactions, and Polymorphic Phase Transition Behavior. Cryst. Growth Des. 2013, 13, 4110–4117.
- (23) Chowdhury, M.; Kariuki, B. M. Supramolecular assembly in cinnamate structures: The influence of the ammonium ion and halogen interactions. *Cryst. Growth Des.* **2006**, *6*, 774–780.
- (24) Crowther, D.; Chowdhury, M.; Kariuki, B. Layering in cinnamate structures: The role of cations and anion substituents. *J. Mol. Struct.* **2008**, 872, 64–71.
- (25) UV-Enhanced Aluminum Mirror. https://www.thorlabs.de/thorproduct.cfm?partnumber=PF10-03-F01; access date 2019-01-21.
- (26) Schaefer, J.; Stejskal, E. O. Carbon-13 Nuclear Magnetic Resonance of Polymers Spinning at the Magic Angle. *J. Am. Chem. Soc.* 1976, 98, 1031–1032.
- (27) Bennett, A. E.; Rienstra, C. M.; Auger, M.; Lakshmi, K. V.; Griffin, R. G. Heteronuclear Decoupling in rotating solids. *J. Chem. Phys.* **1995**, *103*, 6951–6958.
- (28) Fung, B. M.; Khitrin, A. K.; Ermolaev, K. An Improved Broadband Decoupling Sequence for Liquid Crystals and Solids. *J. Magn. Reson.* **2000**, *142*, 97–101.
- (29) Chandran, C. V.; Bräuniger, T. Efficient heteronuclear dipolar decoupling in solid-state NMR using frequency-swept SPINAL sequences. *J. Magn. Reson.* **2009**, 200, 226–232.
- (30) Opella, S. J.; Frey, M. H. Selection of Nonprotonated Carbon Resonances in Solid-State Nuclear Magnetic Resonance. *J. Am. Chem. Soc.* 1979, 101, 5854–5856.
- (31) van Rossum, B.-J.; Förster, H.; de Groot, H. J. M. High-Field and High-Speed CP-MAS ¹³C NMR Heteronuclear Dipolar-Correlation Spectroscopy of Solids with Frequency-Switched Lee-Goldburg Homonuclear Decoupling. *J. Magn. Reson.* **1997**, 124, 516–519
- (32) Massiot, D.; Fayon, F.; Capron, M.; King, I.; Le Calvé, S.; Alonso, B.; Durand, J.-O.; Bujoli, B.; Gan, Z.; Hoatson, G. Modelling one and two dimensional solid-state NMR spectra. *Magn. Reson. Chem.* **2002**, *40*, 70–76.
- (33) Segall, M. D.; Lindan, P. J. D.; Probert, M. J.; Pickard, C. J.; Hasnip, P. J.; Clark, S. J.; Payne, M. C. First-Principles Simulation: Ideas, Illustrations and the CASTEP Code. *J. Phys.: Condens. Matter* **2002**, *14*, 2717–2744.
- (34) Monkhorst, H. J.; Pack, J. D. Special Points for Brillouin-Zone Integrations. *Phys. Rev. B* **1976**, *13*, 5188–5192.
- (35) Aliev, A. E.; Harris, K. D. M.; Harris, R. K.; Carss, S. A.; Olivieri, A. C. Second-order Quadrupolar Effects for Directly Bonded and Remote ¹³C-^{79/81}Br Spin Pairs in High-resolution ¹³C NMR Spectra of Solids. *J. Chem. Soc., Faraday Trans.* **1995**, *91*, 3167–3176.
- (36) Kanao, S.; Kashino, S.; Haisa, M. Topochemical studies. XIII. Structures of 3-bromocinnamic acid and 3-chlorocinnamic acid. *Acta Crystallogr., Sect. C: Cryst. Struct. Commun.* **1990**, *46*, 2436–2438.
- (37) Zahan, M.; Krautscheid, H.; Haase, J.; Bertmer, M.Photodimerization Kinetics of Cinnamate Salts as Studied by Solid-State NMR. Manuscript in preparation, 1990.
- (38) Jenkins, S. L.; Almond, M. J.; Atkinson, S. D. M.; Drew, M. G. B.; Hollins, P.; Mortimore, J. L.; Tobin, M. J. The kinetics of the $2\pi + 2\pi$ photodimerisation reactions of single-crystalline derivatives of trans-cinnamic acid: A study by infrared microspectroscopy. *J. Mol. Struct.* **2006**, 786, 220–226.
- (39) Savion, Z.; Wernick, D. L. Monomer Environments during the Solid-State Photodimerization of *trans-p-Bromocinnamic Acid. J. Org. Chem.* **1993**, *58*, 2424–2427.
- (40) Montaudo, G.; Caccamese, S.; Librando, V. Photodimers of Cinnamic Acid and Related Compounds. A Stereochemical Study by NMR. *Org. Magn. Reson.* **1974**, *6*, 534–536.